Pressure-induced superconductivity in Eu_<0.5>Ca_<0.5>Fe_2As_2 : Wide zero-resistivity region due to suppression of Eu magnetic order and chemical pressure

Mitsuda, Akihiro
Department of Physics, Kyushu University

Matoba, Tomohiro
Department of Physics, Kyushu University

Ishikawa, Fumihiro
Graduate School of Science and Technology, Niigata University

Yamada, Yuh
Department of Physics, Niigata University

他

出版情報：Journal of the Physical Society of Japan. 79 (7), pp.073704(1)-073704(4), 2010-07.
日本物理学会
バージョン：

Pressure-Induced Superconductivity in $Eu_{0.5}Ca_{0.5}Fe_2As_2$: Wide Zero-Resistivity Region Due to Suppression of Eu Magnetic Order and Chemical Pressure

Akihiro Mitsuda*, Tomohiro Matoba, Fumihiro Ishikawa[1], Yuh Yamada[2], and Hirofumi Wada

Department of Physics, Kyushu University, 6-10-1 Hakozaki, Higashi-ku, Fukuoka 812-8581, Japan
[1]*Graduate School of Science and Technology, Niigata University, Niigata 950-2181, Japan*
[2]*Department of Physics, Niigata University, Niigata 950-2181, Japan*

To clarify competition between FeAs-based superconductivity and antiferromagnetism of Eu^{2+}, and the superconducting properties in $EuFe_2As_2$, we investigated a Ca-substituted sample, $Eu_{0.5}Ca_{0.5}Fe_2As_2$, under high pressure. Under ambient pressure, the sample exhibits a spin-density-wave (SDW) transition at $T_{SDW} = 191$ K and antiferromagnetic order at $T_N = 4$ K, but no evidence of superconductivity down to 2 K. The Ca-substitution certainly weakens the antiferromagnetism. With increasing pressure, T_{SDW} shifts to lower temperature and becomes more unclear. Above 1.27 GPa, pressure-induced superconductivity with zero resistivity is observed at around $T_c = 20$ K. At 2.14 GPa, T_c reaches a maximum value of 24 K and the superconducting transition becomes sharpest. The chemical pressure and the suppression of Eu magnetic order induced by Ca substitution enlarge the zero resistivity region compared to pure $EuFe_2As_2$.

KEYWORDS: Fe-based superconductor, pressure, isovalent substitution, europium, antiferromagnetism

Following the initial discovery by Kamihara et al. that $LaFeAsO_{1-x}F_x$ for $0.05 \leq x \leq 0.12$ is a high-T_c superconductor with $T_c = 26$ K,[1] numerous investigations of Fe-based superconductors have been conducted across the world. A recent study has shown that replacing La with other lanthanides increases the T_c up to 55 K, which is the highest T_c value except those for the high-T_c cuprates.[2] The parent material LaFeAsO crystallizes in a tetragonal ZrCuSiAs-type structure, in which LaO and FeAs layers are stacked alternately, and performs a structural phase transition from tetragonal to orthorhombic symmetry at 155 K[3,4] and a spin-density-wave (SDW) transition at 137 K.[3] Either F-doping or oxygen vacancies, which correspond to electron doping, suppresses these transitions and induces the superconductivity.[1] It is intriguing that, although Fe is a magnetic element that has been considered to be destructive to superconductivity, the FeAs layer plays a key role in giving rise to superconductivity.

A similar superconductivity of $T_c = 38$ K was also found in $Ba_{1-x}K_xFe_2As_2$.[5] This sys-

*E-mail address: 3da@phys.kyushuu-u.ac.jp

tem forms a tetragonal $ThCr_2Si_2$-type structure that consists of alternate stacking of Ba/K layers and FeAs layers similar to those in LaFeAsO. Similarly to LaFeAsO, the parent compound $BaFe_2As_2$ exhibits the SDW transition and the structural transition from tetragonal to orthorhombic *Fmmm* at $T_{SDW} = 140$ K simultaneously.[5,6] Substitution of K for Ba, which corresponds to hole doping, induces the superconductivity, accompanied by collapse of the SDW and structural transition.[5] Similar behavior is also observed in AFe_2As_2 (A=Ca,[7] Sr,[8] Eu[9]). In addition, applying external pressure[10–14] and/or chemical pressure (isovalent substitution of P for As)[15–17] also induces the superconductivity. In the case of $EuFe_2As_2$, however, Eu^{2+} also has magnetic moment of $\sim 7\mu_B$ and exhibits an antiferromagnetic order (AFM) at 20 K.[18] Resonant X-ray scattering and neutron diffraction confirm that the Eu^{2+} moments align along the a direction with wave vector $\mathbf{k} = (0, 0, 1)$ in terms of the orthorhombic *Fmmm* structure.[19,20] With increasing pressure, the SDW transition is continuously collapsed and a sharp drop in electrical resistivity at 30 K appears at around 2 GPa, which is reminiscent of superconductivity. After the drop, however, the resistivity goes to a finite value (not zero resistivity) at around 20 K, where the AFM occurs.[21] It is speculated that Cooper pairs should be destroyed by a molecular field due to the AFM of Eu^{2+} ions, as is observed in $HoMo_6S_8$[22] and $HoNi_2B_2C$.[23] Terashima et al. have reported that a higher pressure of ~ 2.8 GPa realizes zero resistivity.[24] Very recently, Matsubayashi et al. have observed superconductivity with zero resistivity in a very narrow pressure range of $2.6 \sim 2.7$ GPa.[25] In the present study, to clarify competition between FeAs-based superconductivity and the AFM of Eu^{2+}, and the superconducting properties in $EuFe_2As_2$, we attempted to weaken the molecular field of Eu^{2+} by diluting Eu^{2+} with nonmagnetic isovalent Ca^{2+}, which was accompanied by the application of chemical pressure due to the smaller volume of the Ca^{2+} ion. Additionally, the diluted sample was investigated under high pressure. Recently, Zheng et al. have reported that magnetically weakened $Eu_{1-y}A_yFe_{2-x}Co_xAs_2$(A=Sr and Ba, $x \sim 0.2$) exhibits superconductivity with zero resistivity.[26] Unfortunately, since $AFe_{2-x}Co_xAs_2$ is also a superconductor of $T_c \sim 20$ K,[27,28] it could be produced by segregation of $AFe_{2-x}Co_xAs_2$. Though $CaFe_2As_2$ also exhibits superconductivity under pressure, it is distinguishable because its T_c value is substantially lower than that of $EuFe_2As_2$. In the present study, we report pressure-induced superconductivity (PISC) with zero resistivity in a wide pressure range in $Eu_{0.5}Ca_{0.5}Fe_2As_2$.

The single crystal of $Eu_{0.5}Ca_{0.5}Fe_2As_2$ was grown in a tin flux. A mixture of constituent elements in a ratio of Eu : Ca : Fe : As : Sn = 0.5 : 0.5 : 2 : 2 : 48, which was put into an alumina crucible, was heated at 1000°C for 24 hours in a quartz tube sealed under 1/3-atm Ar gas at room temperature. Subsequently, the mixture was cooled down to 500°C at the rate of −14°C/h and the tin flux was removed by a centrifuge. We obtained many pieces of plate-like single crystals with typical dimensions of $\sim 3 \times 3 \times 0.1$ mm^3. The powder X-ray diffraction pattern at room temperature exhibits a single phase which crystallizes in the

tetragonal $ThCr_2Si_2$-type structure with lattice constants of $a = 3.897$ Å and $c = 12.006$ Å. These values lie almost halfway between $EuFe_2As_2$ ($a = 3.902$ Å and $c = 12.138$ Å) and $CaFe_2As_2$ ($a = 3.886$ Å and $c = 11.776$ Å), which were also synthesized by our group. The lattice constants of both end compounds are in good agreement with those reported in Ref.[10,18] The energy dispersive X-ray (EDX) spectroscopy confirmed that the composition of the sample is almost Eu : Ca : Fe : As = 0.5 : 0.5 : 2 : 2. These results suggest that 50% of Eu atoms are replaced by Ca atoms in a homogeneous manner. Electrical resistivity under high pressure was measured with current flowing in the *ab* plane by using an ac resistance bridge (LR-700; Linear Research) in the temperature range between 4.2 and 280 K. Pressure was generated up to 2.47 GPa by using a piston-cylinder-type pressure cell, which consists of inner (NiCrAl alloy) and outer (CuBe alloy) cylinders. The sample and a tin manometer were placed into a Teflon cell filled with a pressure-transmitting medium consisting of a mixture of two types of Flourinert in a ratio of FC70 : FC77 = 1 : 1. The Teflon cell was inserted into the pressure cell and pressed by pistons made of nonmagnetic tungsten carbide. Magnetization measurement under high pressure was carried out by a SQUID magnetometer (MPMS; Quantum Design) in the temperature range between 2 and 300 K. Pressure was generated by basically the same method as used in the resistivity measurement. Up to 0.8 GPa, we used a pressure cell made of nonmagnetic CuTi alloy and pistons made of zirconia to reduce the magnetization signal from the pressure cell. Many pieces of small single crystals directed randomly were used in the magnetization measurement. To estimate the magnetization of the sample, the magnetization of the pressure cell was subtracted from the measured value. At 1.4 GPa, we measured the magnetization in a field of 1 mT after zero field cooling (ZFC) and field cooling (FC) by using a pressure cell made of CuBe alloy to confirm the Meissner-Ochsenfeld effect and its volume fraction.

Figure 1 demonstrates the temperature dependence of the electrical resistivity ρ of $Eu_{0.5}Ca_{0.5}Fe_2As_2$ under various pressures. In addition, the ρ–T curves of $CaFe_2As_2$ and $EuFe_2As_2$ synthesized by our group, the T_{SDW} of which are 170 K and 191 K, respectively, are also shown in the inset. These curves qualitatively coincide with those reported in Ref.[10,18,29] The behavior of $Eu_{0.5}Ca_{0.5}Fe_2As_2$ under ambient pressure is intermediate between those of the two end compounds. A sharp cusp, which corresponds to spin-density-wave (SDW) transition, is observed at $T_{SDW} = 191$ K. The T_{SDW} is similar to that of $EuFe_2As_2$,[18] but the shape of the cusp is similar to that of $CaFe_2As_2$.[29] Below T_{SDW}, with decreasing temperature, the resistivity decreases significantly with a concave-up curvature down to 70 $\mu\Omega$cm without any anomalies such as the superconductivity or AFM of Eu^{2+}. Unlike in the case of $Eu_{0.5}K_{0.5}Fe_2As_2$,[9] substitution of isovalent Ca for Eu neither collapses the SDW transition nor induces superconductivity. At 0.43 and 0.63 GPa, except for the depression of T_{SDW}, the temperature dependence of ρ is qualitatively the same as that at ambient pressure. At

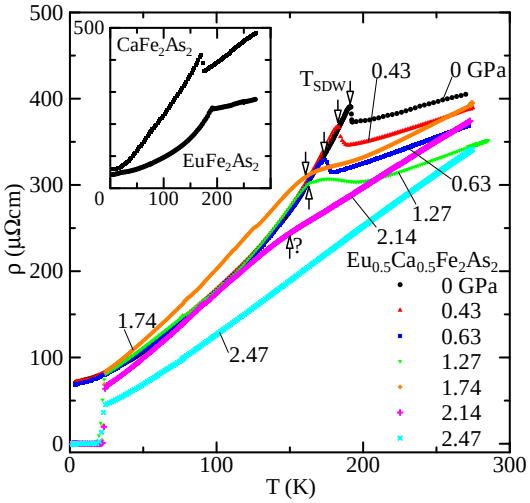

Fig. 1. (Color online) Electrical resistivity versus temperature of $Eu_{0.5}Ca_{0.5}Fe_2As_2$ at various pressures. The open arrows depict the spin-density-wave (SDW) temperature, T_{SDW}. However, T_{SDW} is difficult to determine at 2.14 GPa. The inset exhibits the temperature dependence of the resistivity of $CaFe_2As_2$ and $EuFe_2As_2$ synthesized by our group.

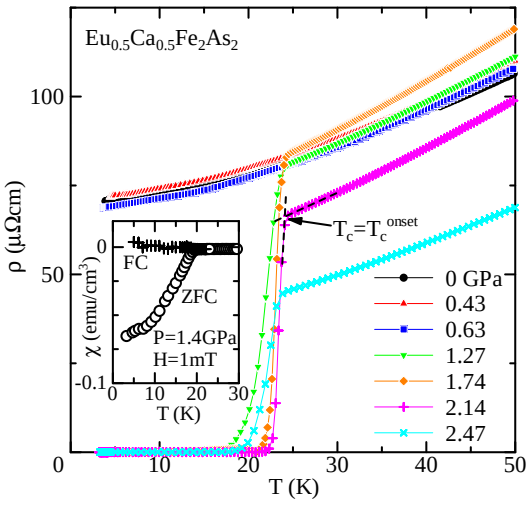

Fig. 2. (Color online) Electrical resistivity versus temperature of $Eu_{0.5}Ca_{0.5}Fe_2As_2$ at various pressures in the low temperature region. The short dashed line shows how to define the onset superconducting temperature, T_c^{onset}. The inset demonstrates the magnetic susceptivility measured in a field of 1 mT at 1.4 GPa after ZFC (open circle) and FC (cross).

1.27 GPa, superconductivity with zero resistivity suddenly emerges at around 23 K, which is accompanied by a broadening of the SDW transition. The ρ–T curve is comparably similar to that below 0.63 GPa except for the superconducting behavior and the shape of the curve at T_{SDW}, which implies this pressure is close to critical pressure P_c. At 1.74 GPa, as shown in Fig. 2, the superconducting transition becomes sharper than that at 1.27 GPa, which suggests

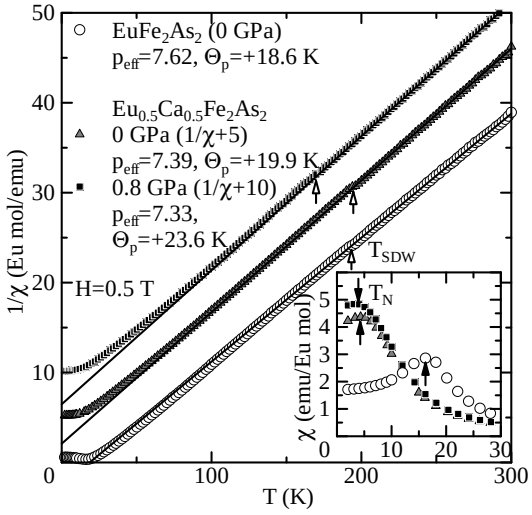

Fig. 3. Inverse susceptibility versus temperature of $EuFe_2As_2$ at 0 GPa and of $Eu_{0.5}Ca_{0.5}Fe_2As_2$ at 0 and 0.8 GPa. The open arrows depict spin-density-wave (SDW) temperature. The solid lines correspond to the best fit to the Curie-Weiss law. The inset demonstrates the temperature dependence of magnetic susceptibility in the low temperature region. The solid arrows show the Néel temperature.

more homogeneous superconductivity. The anomaly associated with the SDW transition becomes broader and more indistinct. The slope of the ρ–T curve above $T_{\rm SDW}$ becomes larger. These features result in considerable change of the shape of the ρ–T curve. At 2.14 GPa, the sharp superconducting transition shifts to a slightly higher temperature, which demonstrated a maximum $T_{\rm c}$ of 24 K in the present study. The anomaly of the SDW transition can be seen as a slight convex-up behavior at around 150 K, but is too shallow to determine the $T_{\rm SDW}$ value precisely. The residual resistivity ρ_0, which is determined as the ρ value just above $T_{\rm c}$, begins to drop. Finally, at 2.47 GPa, the transition again becomes less sharp and shifts to lower temperature, which is possibly the onset of collapse of the superconductivity. The ρ–T curve above $T_{\rm c}$ exhibits concave-up behavior and no anomaly, which indicates the SDW transition is collapsed completely. The ρ_0 value decreases to $\sim 45\,\mu\Omega$cm. A similar behavior with pressure is also observed in AFe_2As_2 (A=Ca, Sr, Ba).[11,13,14,30] Recently, some groups have pointed out that partial superconductivity is often induced by inhomogeneous and/or uniaxial pressure in the Fe-based systems.[31–33] To confirm bulk superconductivity, the magnetization in a field of 1 mT was measured at 1.4 GPa after ZFC and FC, as shown in the inset of Fig. 2. A clear decrease in the magnetic susceptivility χ is observed after ZFC below $\sim$ 20 K. The χ value reaches to $\sim$ 75% of $-1/(4\pi) = -0.080$ emu/cm^3 at 5 K. These results indicate that the bulk superconductivity occurs.

Figure 3 shows the temperature dependence of the inverse magnetic susceptibility $1/\chi$ of $EuFe_2As_2$ at 0 GPa and of $Eu_{0.5}Ca_{0.5}Fe_2As_2$ at 0 and 0.8 GPa. The inset indicates the

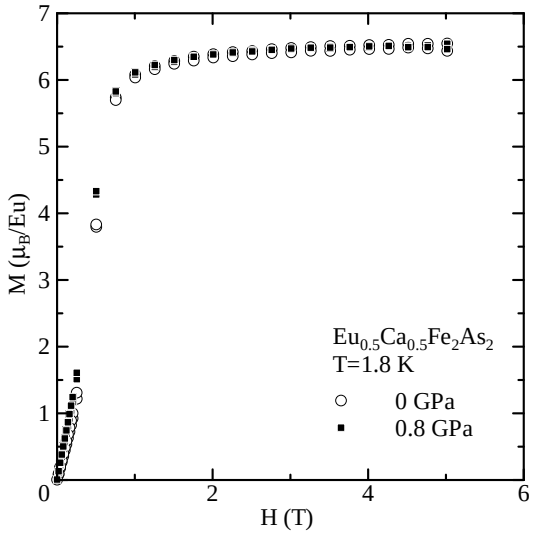

Fig. 4. Magnetization curves at 1.8 K of $Eu_{0.5}Ca_{0.5}Fe_2As_2$for 0 and 0.8 GPa.

χ–T curves in the low temperature region. For $EuFe_2As_2$, the data is almost in accordance with that previously reported.[18] There exists a clear peak in the χ–T curve at T_N = 17 K and a kink in the $1/\chi$–T curve at T_{SDW} = 193 K. Above T_{SDW}, the susceptibility obeys the Curie-Weiss (CW) law with an effective moment p_{eff} of 7.62μ_B/Eu and a Weiss temperature Θ_p of +18.6 K. The p_{eff} value is close to the theoretical value (7.94μ_B/Eu) of a free Eu^{2+} ion. The positive Θ_p value suggests dominant ferromagnetic exchange interactions in spite of the AFM of Eu^{2+} with $\mathbf{k} = (0, 0, 1)$ confirmed by the resonant X-ray scattering and the neutron diffraction.[19,20] Actually, a comparably small magnetic field of $\sim$ 1 T can saturate magnetization.[18] Replacing 50% Eu ions with Ca ions results in almost full retention of the CW behavior, but lowers the T_N to 4 K. The former implies that the Eu valence remains almost 2+. The latter means that the AFM is destabilized, which results from depression of the RKKY (Ruderman-Kasuya-Kittel-Yosida) interaction due to dilution of magnetic Eu^{2+} ions. We also examined the magnetization in a field of 0.02 T after ZFC and FC (not shown). Since these data are exactly the same, the peak at around 4 K is not ascribed to spin glass. By applying pressure to $Eu_{0.5}Ca_{0.5}Fe_2As_2$, T_{SDW} is lowered, but the T_N value and the CW behavior, which are associated with Eu^{2+}, are nearly unchanged. This means that the valence and the magnetism of Eu are insensitive to pressure. We also measured the magnetization curves at 1.8 K as shown in Fig. 4. At both 0 and 0.8 GPa, the magnetization is saturated to 6.5μ_B/Eu, which is close to the magnetic moment of Eu^{2+} of 7μ_B/Eu. This also supports the idea that the Eu valence remains close to 2+ under pressures up to 0.8 GPa. We speculate that the magnetism and the valence of Eu are probably also preserved under pressures higher than 0.8 GPa. To investigate competition between the magnetism of Eu and the superconductivity in more detail, magnetization measurements under higher pressure are now in progress.

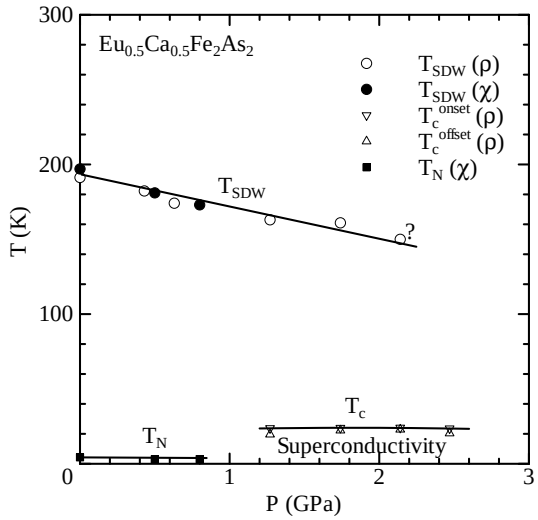

Fig. 5. Temperature versus pressure phase diagram of $Eu_{0.5}Ca_{0.5}Fe_2As_2$. The T_c^{onset} value has a faint maximum of 24 K at around 2.14 GPa.

To summarize the present experiments, the T–P phase diagram is shown in Fig. 5. We define T_c^{offset} as the temperature at which the resistivity reaches 10% of the residual resistivity ρ_0. During the suppression of T_{SDW} with increasing pressure, the superconductivity with zero resistivity of $T_c \sim 20$ K emerges suddenly at around 1.2 GPa. The pressure dependence of T_c is quite small but has a faint maximum of 24 K at around 2.14 GPa, where the superconducting transition is the sharpest. The AFM of Eu^{2+} is realized at around 4 K. Since T_N is much lower than T_c, it seems that the superconductivity with zero resistivity is stabilized in a wide pressure range unlike in the case of $EuFe_2As_2$.[25)]

Compared with those in $CaFe_2As_2$ ($P_c \sim 0.4$ GPa and $T_c \sim 10$ K[11,30)]), the P_c and T_c in $Eu_{0.5}Ca_{0.5}Fe_2As_2$ are substantially higher ($P_c \sim 1.27$ GPa and $T_c \sim 24$ K), which indicates that the observed superconductivity is intrinsic, not due to an impurity such as $CaFe_2As_2$. Though a structural phase transition from tetragonal to collapsed tetragonal type takes place above 0.8 GPa in $CaFe_2As_2$,[11,30)] there exists no evidence of such a structural transition under high pressures up to 2.47 GPa in $Eu_{0.5}Ca_{0.5}Fe_2As_2$. On the other hand, compared with those of $EuFe_2As_2$ ($P_c \sim 2.0$ GPa and $T_c \sim 30$ K),[21)] both P_c and T_c were lower in the present system. Since the lattice volume of $Eu_{0.5}Ca_{0.5}Fe_2As_2$ was 1.4% smaller than that of $EuFe_2As_2$, it seems likely that chemical pressure was applied in addition to external pressure in the present system. Jørgensen et al. have examined the pressure dependence of lattice constants of $BaFe_2As_2$ and fit their results to the Birch-Murnaghan equation of state.[34)] Assuming that their fitting results are applicable to the present system, a volume contraction of 1.4% through the substitution of Ca ions for 50% of the Eu ions corresponds to a pressure of ~ 1 GPa. This chemical pressure plus P_c (1.27 GPa) for $Eu_{0.5}Ca_{0.5}Fe_2As_2$ is reasonably close to the P_c (2.0 GPa) for $EuFe_2As_2$.[21)] Dilution of Eu^{2+}, which reduces not only T_N but

also T_c, is less effective at decreasing T_c than T_N.

It has been pointed out that the AFM of Eu^{2+} is also weakened in $Eu_{0.5}K_{0.5}Fe_2As_2$,[35] where the K-doping corresponds to simultaneous hole doping and weakening of AFM of Eu^{2+}. In the present system, the application of pressure may have corresponded to carrier doping, and substitution of Ca may have corresponded to the weakening of the AFM of Eu^{2+}, which means the two effects can be controlled independently. Thus, $Eu_{1-x}Ca_xFe_2As_2$ is a good candidate for investigating competition between the FeAs-based superconductivity and the AFM of Eu^{2+}.

Finally, the chemical and external pressures are also expected to induce a valence transition from Eu^{2+} ($J = 7/2$, magnetic) toward Eu^{3+} ($J = 0$, non-magnetic), because Eu^{2+} has a larger volume than Eu^{3+}. However, the effective magnetic moment and the spontaneous magnetization remain the values for an Eu^{2+} ion under pressures up to 0.8 GPa in the present system. There was no evidence of an Eu valence change in the present study.

In conclusion, we observed pressure-induced bulk superconductivity ($T_c \sim 24$ K) with zero resistivity of $Eu_{0.5}Ca_{0.5}Fe_2As_2$ in an extended pressure range of $P = 1.27 \sim 2.47$ GPa. Diluting Eu with isovalent Ca weakens the AFM of Eu^{2+} and induces a chemical pressure of ~ 1 GPa, which both results in a widening of the zero resistivity region. Substitution of Ca and/or applying pressure seem not to change the Eu valence.

Acknowledgments

The authors thank Dr. M. Watanabe at the Center of Advanced Instrumental Analysis, Kyushu University for helping us perform SEM-EDX analysis.

References

1) Y. Kamihara, T. Watanabe, M. Hirano, and H. Hosono: J. Am. Chem. Soc. **130** (2008) 3296.
2) X. F. Chen, T. Wu, G. Wu, R. H. Liu, H. Chen, and D. F. Fang: Nature (London) **453** (2008) 761.
3) C. de la Cruz, Q. Huang, J. W. Lynn, J. Li, W. Ratcliff II, H. A. Mook, G. F. Chen, J. L. Luo, N. L. Wang, and Pengcheng Dai: Nature (London) **453** (2008) 899.
4) T. Nomura, S.W. Kim, Y. Kamihara, M. Hirano, P. V. Sushko, K. Kato, M. Takata, A. L. Shluger, and H. Hosono: Supercond. Sci. Technol. **21** (2008) 125028.
5) M. Rotter, M. Tegel, and D. Johrendt: Phys. Rev. Lett. **101** (2008) 107006.
6) M. Rotter, M. Tegel, and D. Johrendt, I. Schellenberg, W. Hermes, and R. Pöttgen: Phys. Rev. B **78** (2008) 020503(R).
7) G. Wu, H. Chen, T. Wu, Y. L. Xie, Y. J. Yan, R. H. Liu, X. F. Wang, J. J. Ying, and X. H. Chen: J. Phys.: Condens. Matter **20** (2008) 422201.
8) K. Sasmal, B. Lv, B. Lorenz, A. M. Guloy, F. Chen, Y. Y. Xue, and C. W. Chu: Phys. Rev. Lett. **101** (2008) 107007.
9) H. S. Jeevan, Z. Hossain, Deepa Kasinathan, H. Rosner, C. Geibel, and P. Gegenwart: Phys. Rev. B **78** (2008) 092406.
10) T. Park, E. Park, H. Lee, T. Klimczuk, E. D. Bauer, F. Ronning, and J. D. Thompson: J. Phys.: Condens. Matter **20** (2008) 322204.
11) M. S. Torikachvili, S. L. Bud'ko, N. Ni, and P. C. Canfield: Phys. Rev. Lett. **101** (2008) 057006.
12) P. L. Alireza, Y. T. C. Ko, J. Gillett, C. M. Petrone, J. M. Cole, G. G. Lonzarich, and S. E. Sebastian: J. Phys.: Condens. Matter **21** (2009) 012208.
13) H. Kotegawa, H. Sugawara, and H. Tou: J. Phys. Soc. Jpn. **78** (2009) 013709.
14) F. Ishikawa, N. Eguchi, M. Kodama, K. Fujimaki, M. Einaga, A. Ohmura, A. Nakayama, A. Mitsuda, and Y. Yamada: Phys. Rev. B **79** (2009) 172506.
15) Z. Ren, Q. Tao, S. Jiang, C. Feng, C. Wang, J. Dai, G. Cao, and Z. Xu: Phys. Rev. Lett. **102** (2009) 137002.
16) S. Jiang, H. Xing, G. Xuan, C. Wang, Z. Ren, C. Feng, J. Dai, Z. Xu, and G. Cao: J. Phys.: Condens. Matter **21** (2009) 382203.
17) S. Kasahara, T. Shibauchi, K. Hashimoto, K. Ikada, S. Tonegawa, H. Ikeda, H. Takeya, K. Hirata, T. Terashima, and Y. Matsuda: arXiv:0905.4427.
18) Z. Ren, Z. Zhu, S. Jiang, X. Xu, Q. Tao, C. Wang, C. Feng, G. Cao, and Z. Xu: Phys. Rev. B **78** (2008) 052501.
19) J. Herrero-Martin, V. Scagnoli, C. Mazzoli, Y. Su, R. Mittal, Y. Xiao, T. Brueckel, N. Kumar, S. K. Dhar, A. Thamizhavel, and L. Paolasini: Phys. Rev. B **80** (2009) 134411.
20) Y. Xiao, Y. Su, M. Meven, R. Mittal, C. M. N. Kumar, T. Chatterji, S. Price, J. Persson, N. Kumar, S. K. Dhar, A. Thamizhavel, and Th. Brueckel: arXiv:0908.3142.
21) C. F. Miclea, M. Nicklas, H. S. Jeevan, D. Kasinathan, Z. Hossain, H. Rosner, P. Gegenwart, C. Geibel, and F. Steglich: Phys. Rev. B **79** (2009) 212509.
22) M. Ishikawa and Ø. Fischer: Solid State Commun **23** (1977) 37.
23) H. Eisaki, H. Takagi, R. J. Cava, B. Batlogg, J. J. Krajewski, W. F. Peck, Jr., K. Mizuhashi, J. O. Lee, and S. Uchida: Phys. Rev. B **50** (1994) 647.
24) T. Terashima, M. Kimata, H. Satsukawa, A. Harada, K. Hazama, S. Uji, H. S. Suzuki, T. Matsumoto,

and K. Murata: J. Phys. Soc. Jpn. **78** (2009) 083701.

25) K. Matsubayashi: private communication

26) Y. He, T. Wu, G. Wu, Q. J. Zheng, Y. Z. Liu, H. Chen, J. J. Ying, R. H. Liu, X. F. Wang, Y. L. Xie, Y. J. Yan, J. K. Dong, S. Y. Li, and X. H. Chen: J. Phys. : Condens. Matter **22** (2010) 235701.

27) A. S. Sefat, R. Jin, M. A. McGuire, B. C. Sales, D. J. Singh, and D. Mandrus: Phys. Rev. Lett. **101** (2008) 117004.

28) A. Leithe-Jasper, W. Schnelle, C. Geibel, and H. Rosner: Phys. Rev. Lett. **101** (2008) 207004.

29) N. Ni, S. Nandi, A. Kreyssig, A. I. Goldman, E. D. Mun, S. L. Bud'ko, and P. C. Canfield: Phys. Rev. B **78** (2008) 014523.

30) H. Lee, E. Park, T. Park, V. A. Sidorov, F. Ronning, E. D. Bauer, and J. D. Thompson: Phys. Rev. B **80** (2009) 024519.

31) W. Yu, A. A. Aczel, T. J. Williams, S. L. Bud 'ko, N. Ni, P. C. Canfield, and G. M. Luke: Phys. Rev. B **79** (2009) 020511(R).

32) H. Kotegawa, T. Kawazoe, H. Sugawara, K. Murata, and H. Tou: J. Phys. Soc. Jpn. **78** (2009) 083702.

33) T. Yamazaki, N. Takeshita, R. Kobayashi, H. Fukazawa, Y. Kohori, K. Kihou, C. Lee, H. Kito, A. Iyo, and H. Eisaki: arXiv:1003.0913.

34) J. -E. Jørgensen, J. S. Olsen, and L Gerward: Solid State Commun. **149** (2009) 1161.

35) Anumpam, P. L. Paulose, H. S. Jeevan, C. Geibel, and Z. Hossain: J. Phys.: Condens. Matter **21** (2009) 265701.